20th International Conference on Renewable Energies and Power Quality (ICREPQ'22)
Vigo (Spain), 27th to 29th July 2022
Renewable Energy and Power Quality Journal (RE&PQJ)
ISSN 2172-038 X, Volume No.20, September 2022

A wavelet packet-dual fuzzy control method for hybrid energy storage to suppress wind power fluctuations

Lv. Huixiang[1], Chen. Caixue[2] and Xiong. Zhigang[1]

[1] Department of Energy Powertrain
Xiangtan University
Xiangtan, China
Phone/Fax number: +0086 17673911062, e-mail: mia05010104@outlook.com

[2] Department of Energy Powertrain
Xiangtan University
Xiangtan, China
Phone/Fax number: +0086 15200376559, e-mail: 201921002042@smail.xtu.edu.cn

Abstract. In order to smooth the wind power output, a wavelet packet-double fuzzy control for hybrid energy storage is proposed to smooth the wind power fluctuation. Firstly, the wavelet packet decomposition is used to decompose the wind power output to obtain the grid-connected power signal and the power signal allocated to the hybrid energy storage. Then, the double fuzzy control algorithm is used to optimise the hybrid energy storage SOC to maintain it within a reasonable range, and to make a secondary correction to the hybrid energy storage power allocation, taking into account the charge states of lithium batteries and super capacitors. The results of the analysis show that the proposed method can smooth out the wind power fluctuations while keeping the energy storage SOC within a reasonable range.

Key words. Wind power generation, Power fluctuation, Mixed energy storage, Wavelet packet decomposition, Double fuzzy control;

1. Introduction

As a clean and renewable energy source, wind energy is developing rapidly in countries around the world. As wind power is delivered to the grid on a large scale, its fluctuating, intermittent and random characteristics have a more and more significant impact on the stability and reliability of the power system [1], a factor that largely limits the development of wind power.

With the rapid development of energy storage technology, the configuration of energy storage systems with a certain capacity on the power generation side can largely stabilize wind power fluctuations. Energy-based energy storage has the advantages of high energy density and strong storage capacity, but also has disadvantages such as low power density and short cycle life; power-based energy storage has the advantages of fast response speed and high-power density, but low energy density [2], using hybrid energy storage systems to cooperate with each other can achieve complementary advantages of both. In the literature [3], a zero-phase low-pass filter-based power fluctuation control strategy for hybrid energy storage smoothing direct-drive wind turbines was developed to overcome the low-pass filter phase lag problem and improve the resolution of detecting high, medium and low frequency power. The literature [4] used moving average filtering to obtain the reference power of the hybrid energy storage system and variable modal decomposition (VMD) to obtain the initial power distribution of the hybrid energy storage. In the literature [5], an initial power allocation based on empirical modal decomposition (EMD) is proposed, and a fuzzy control based on power command correction and a control strategy based on SOC optimization are proposed considering real-time and future SOC levels. In the literature [6], a reference power and capacity allocation method for obtaining hybrid energy storage using sliding average and empirical modal decomposition EMD is proposed to smooth out wind power fluctuations in real time with the objective of highest net benefit. The literature [7] proposed a Model Predictive Control (MPC) based controller to smooth the wind power output generated by wind farms and subject to various constraints of the system model. In the literature [8], a multi-scale wavelet packet decomposition of the wind power is performed to give a smoother power command to the BESS, which effectively extends the operational lifetime of the device, but the optimization of the SOC of the energy storage device is not further investigated in the paper. The literature [9] the adaptive wavelet packet decomposition method for smoothing wind power fluctuations is proposed, and the power command of the battery and the supercapacitor is corrected twice by using fuzzy optimal control according to the charge state of the supercapacitor, but the charge state of the battery is not considered.

In this paper, a wavelet packet-double fuzzy control hybrid energy storage method is proposed to suppress the fluctuation of wind power. First, the wavelet packet decomposition is used to obtain the wind power grid-connected power and the hybrid energy storage power; finally, The SOC of the hybrid energy storage is optimised by means of a fuzzy control algorithm to keep it within a reasonable range and to correct the charging and discharging power of the hybrid energy storage twice. The analysis results of the example verify the effectiveness of the method proposed in this paper.

2. Wavelet Packet Decomposition for Power Allocation

Wavelet packet decomposition is suitable for decomposing non-stationary signals. Compared with wavelet decomposition, wavelet packet decomposition decomposes the signal more finely, divides the time-frequency plane more carefully, and has higher resolution for the high-frequency part of the signal, and wavelet packet decomposition can choose the frequency band that matches the signal spectrum according to the characteristics of the signal being analysed, which can better analyse the signal. Wavelet packet decomposition of the original signal, to obtain the high-frequency signal and low-frequency signal, and then the decomposition of the decomposed high-frequency signal and low-frequency signal in the decomposition, until the decomposition requirements. The 6-layer wavelet packet decomposition tree shown in Fig.1 is used as an example to illustrate.

Assuming that the wind power output is P, a 6-layer wavelet packet decomposition is performed, and the decomposition algorithm is as follows:

$$\begin{cases} P_{6,0}^{n} = \sum\limits_{k} h_{k-2l} P_{5,0} \\ P_{6,1}^{n} = \sum\limits_{k} g_{k-2l} P_{5,0} \end{cases} \tag{1}$$

The 6-layer wavelet packet reconstruction algorithm is:

$$\begin{cases} P_{6,0} = \sum\limits_{k} \left(\tilde{h}_{l-2k} P_{6,0}^{2n} + \tilde{g}_{l-2k} P_{6,0}^{2n+1} \right) \\ P_{6,1} = \sum\limits_{k} \left(\tilde{h}_{l-2k} P_{6,1}^{2n} + \tilde{g}_{l-2k} P_{6,1}^{2n+1} \right) \end{cases} \tag{2}$$

$P_{6,0}^{n}$ 、 $P_{6,1}^{n}$ 、 $P_{6,0}^{2n+1}$ 、 $P_{6,1}^{2n+1}$ are the low and high frequency coefficients before and after the reconstruction of the 6-layer decomposition, respectively, n is the number of decomposition levels; h_{k-2l} 、 g_{k-2l} 、 $\tilde{h}_{l-2k}$ 、 $\tilde{g}_{l-2k}$ are the filter coefficients of the wavelet packet decomposition before and after reconstruction, respectively. $P_{6,0}$ 、 $P_{6,1}$ are the low and high frequency power signals reconstructed from layer 6 wavelet packets.

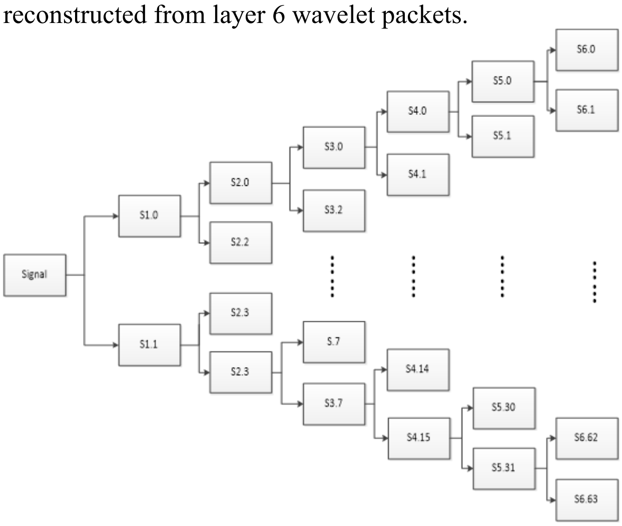

Fig.1 Schematic diagram of wavelet packet decomposition

In Fig.1, Signal is the original signal to be decomposed, P1.0 and P1.1 are the low-frequency signal and high-frequency signal of the first layer, respectively. The signal of the first layer is further decomposed into a high frequency signal and a low frequency signal to obtain the signal of the second layer, and so on.

The simulation example in this paper uses the 24-hour actual output power data of a 70 MW wind farm, and the sampling time is 30 s, as shown in Fig. 2. DB8 wavelet basis function is better in non-smooth vibration signal analysis[10], so DB8 wavelet is used to decompose 6-layer wavelet packets for wind farm output power signal. By performing a fast Fourier transform on the wind farm output power data, the amplitude-frequency information of the data is obtained and analysed to determine the power component of the first frequency band as the grid-connected power**,** as shown in Fig.3; the power component of the 2-4 frequency band as the battery charging and discharging power reference command, as shown in Fig.4; the power component of the remaining 5-64 frequency bands as the supercapacitor charging and discharging power reference command, as shown in Fig. 5. The expression of power distribution is obtained as follows:

$$\begin{Bmatrix} P(t) = P_{grid}(t) + P_b(t) + P_c(t) \\ P_{grid}(t) = P_0(T) \\ P_b(t) = P_1(t) + P_2(t) + P_3(t) \\ P_c(t) = P_4(t) + P_5(t) + \cdots + P_{63}(t) \end{Bmatrix} \tag{3}$$

$P_{grid}(t)$ is the grid-connected power at time t; $P_c(t)$ is the charge and discharge power of the supercapacitor at time t; $P_b(t)$ is the charge and discharge power of the lithium battery at time t.

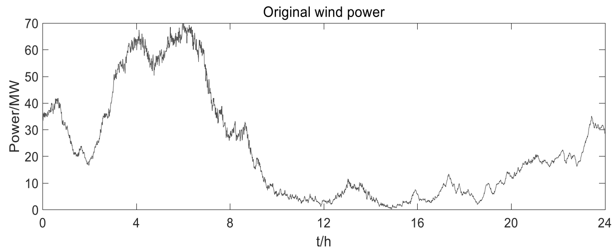

Fig. 2. Original wind power output power

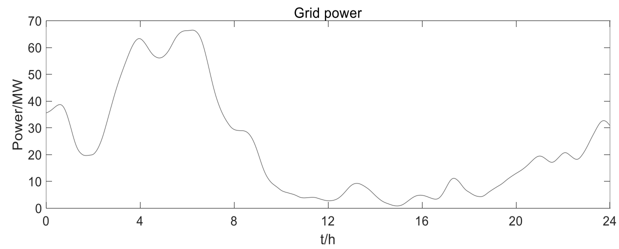

Fig. 3 Grid-connected power

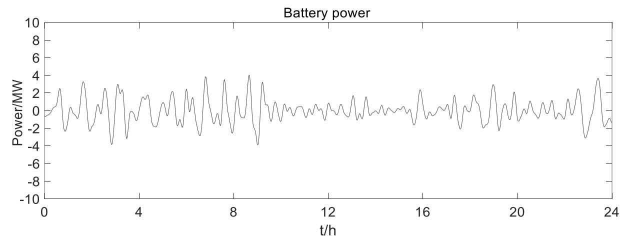

Fig. 4. Lithium battery charge and discharge power

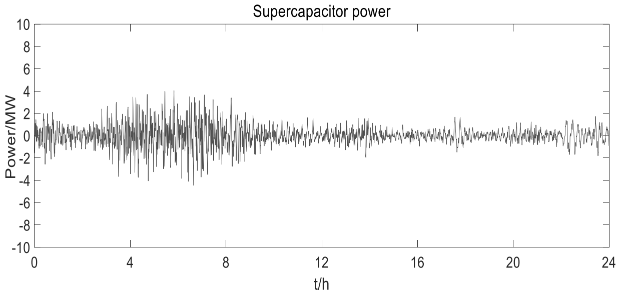

Fig. 5. Supercapacitor charging and discharging power

3. Energy Storage Model

The energy change of the supercapacitor and lithium battery can be obtained by integrating the charging and discharging power of the energy storage, which can be expressed as[11]:

$$\begin{cases} E_c(t) = E_c(t-1) + \int_0^T P_c(t)\,dt \\ E_b(t) = E_b(t-1) + \int_0^T P_b(t)\,dt \end{cases} \tag{4}$$

$E_c(t)$ is the capacity of the supercapacitor at time t, and $E_b(t)$ is the capacity of the lithium battery at time t, T is the sampling time.

The real-time *SOC* of supercapacitor and lithium battery is expressed as follows[12]:

$$\begin{cases} SOC_c(t) = SOC_{c0} + \frac{E_c(t)}{E_{mc}} \\ SOC_b(t) = SOC_{b0} + \frac{E_b(t)}{E_{mb}} \end{cases} \tag{5}$$

SOC_{c0} and SOC_{b0} are the initial charge of the supercapacitor and lithium battery respectively, E_{mc} and E_{mb} are the rated capacity of the supercapacitor and lithium battery respectively.

The state of charge SOC of the supercapacitor and lithium battery during operation cannot exceed the limit, so the rated capacity of the supercapacitor and lithium battery must satisfy the equation:

$$\begin{cases} E_{mc} = \frac{2*max\{\max(E_c), -\min(E_c)\}}{\eta_{c*}(SOC_{cmax}-SOC_{cmin})} \\ E_{mb} = \frac{2*max\{\max(E_b), -\min(E_b)\}}{\eta_{b*}(SOC_{bmax}-SOC_{bmin})} \end{cases} \tag{6}$$

η_b and η_c are the energy conversion efficiencies of supercapacitor and lithium battery, taking 85% and 95% respectively [12]; SOC_{cmax} 、 SOC_{bmax} 、 SOC_{cmin} 、 SOC_{bmin} are the maximum and minimum values of the supercapacitor and lithium battery, taking 1 and 0 respectively.

4. Fuzzy Control of Energy Storage SOC

A. System Control Strategy

The complementary characteristics of hybrid energy storage composed of supercapacitors and lithium batteries compensate for the shortcomings of single types of energy storage and optimise the fluctuation smoothing effect on the time scale and power scale. However, the hybrid energy storage power allocation based on wavelet packet decomposition theory alone may cause overcharging and discharging of energy storage in actual operation, which not only shortens the life of energy storage devices but also affects the final smoothing performance. Based on this, this paper adopts a double fuzzy control algorithm to optimise the hybrid energy storage SOC and e-correct the allocated hybrid energy storage charging and discharging power to maintain the SOC of supercapacitor and lithium battery within a reasonable range, so as to achieve the effect of optimising the hybrid energy storage output. The control strategy is shown in the Fig. 6 shown.

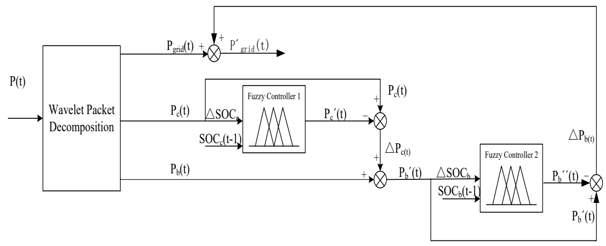

Fig. 6 Control strategy

As shown in Fig.6. First, the original power $P_w(t)$ of the wind power output at time t is decomposed by the wavelet packet to obtain the grid-connected power $P_{grid}(t)$ and the hybrid energy storage power reference commands $P_b(t)$ and $P_c(t)$.According to the characteristics of each energy storage, the lithium battery obtains the low-frequency power component, and the supercapacitor obtains the high-frequency power component. The hybrid energy storage SOC is optimized by adding a double fuzzy control algorithm, which corrects the allocated storage power twice. Fuzzy controller 1 obtains the corrected supercapacitor charge and discharge power as $P_c'(t)$; The charge and discharge power of the lithium battery after the correction obtained by the fuzzy controller 2 is $P_b''(t)$; the grid-connected power after two fuzzy control corrections is $P_{grid}'(t)$.

B. Fuzzy Controller 1

Supercapacitor state-of-charge change ΔSOC_c at time t and the state of charge $SOC_c(t-1)$ of the supercapacitor at time t-1 are used as the input of the fuzzy control, and the output is the power adjustment coefficient $k1$ of the supercapacitor. The corrected charge-discharge power of the supercapacitor and lithium battery is:

$$\begin{cases} P_c'(t) = k1 * P_c(t) \\ P_b'(t) = P_b(t) + (1-k1) * P_c(t) \end{cases} \tag{7}$$

The design of the fuzzy rules follows the following principles: when the state of charge $SOC_c(t)$ of the supercapacitor is small and needs to be discharged at the next moment, or when the state of charge $SOC_c(t)$ of the supercapacitor is large and needs to be charged at the next moment, then reduce the charge and discharge of the supercapacitor and allocate a part of the power to the lithium battery.

Input 1: ΔSOC_c;The input range is [-1,1], and the fuzzy domain is {-10, -9, -8, -7, -6, -5, -4, -3, -2, -1,0,1,2, 3, 4, 5, 6, 7, 8, 9, 10}, and the fuzzy subsets is{NB, NM, NS, PS, PM, PB}.

Input 2: $SOC_c(t-1)$;The input range is [0,1], the fuzzy universe is {0,1,2,3,4,5,6,7,8,9,10}, and the fuzzy subset is {NB, NM, NS, PS, PM, PB}.

Output: $k1$; The input range is [0,1], the fuzzy universe is {0,1,2,3,4,5,6,7,8,9,10}, and the fuzzy subset is {NB, NM, NS, PS, PM, PB}.

The input and output membership functions and fuzzy control rules of the fuzzy controller 1 are shown in Fig. 7, Fig. 8 and Table I respectively.

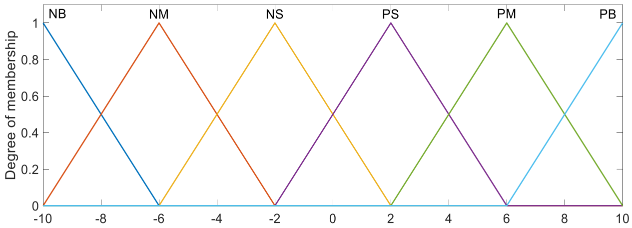

(a) Membership function of ΔSOC_c

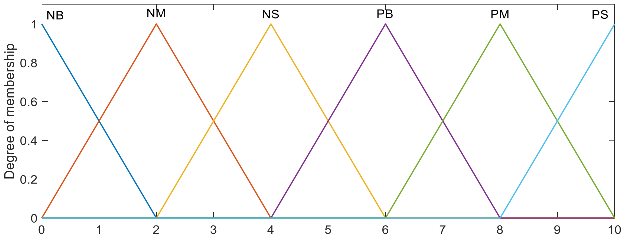

(b) Membership function of $SOC_c(t-1)$

Fig. 7. Fuzzy control input membership function

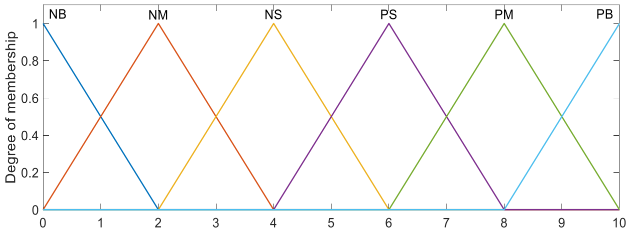

Fig. 8. Fuzzy control output membership function

Table I. Fuzzy control rule

ΔSOC_c	$SOC_c(t-1)$					
	NB	**NM**	**NS**	**PS**	**PM**	**PB**
NB	NB	NM	NS	PS	PM	PB
NM	NM	NS	PS	PM	PB	PB
NS	NS	PS	PM	PB	PB	PB
PS	PB	PB	PB	PM	PS	NS
PM	PB	PB	PM	PS	NS	NM
PB	PB	PM	PS	NS	NM	NB

C. Fuzzy Controller 2

Battery state-of-charge change ΔSOC_b at time t and the state of charge $SOC_b(t-1)$ of the battery at time t-1 are used as the input of the fuzzy control , and the output is the power adjustment coefficient $k2$ of the battery. The corrected lithium battery charging and discharging power and grid-connected power are:

$$\begin{Bmatrix} P_b''(t) = k2 * P_b'(t) \\ P_{grid}'(t) = P_{grid}(t) + (1-k2) * P_b'(t) \end{Bmatrix} \quad (8)$$

The design of the fuzzy rules follows the following principles: when the state of charge $SOC_b(t)$ of the supercapacitor is small and needs to be discharged at the next moment, or when the state of charge $SOC_b(t)$ of the supercapacitor is large and needs to be charged at the next moment, then reduce the charge and discharge of the lithium battery and allocate a part of the power to the grid.

Input 1: ΔSOC_b;The input range is [-1,1], and the fuzzy domain is {-10, -9, -8, -7, -6, -5, -4, -3, -2, -1,0,1,2, 3, 4, 5, 6, 7, 8, 9, 10}, and the fuzzy subsets is {NB, NM, NS, PS, PM, PB}.

Input 2: $SOC_b(t-1)$;The input range is [0,1], the fuzzy universe is {0,1,2,3,4,5,6,7,8,9,10}, and the fuzzy subset is {NB, NS, ZO, PS, PB}.

Output: $k2$; The input range is [0,1], the fuzzy universe is {0,1,2,3,4,5,6,7,8,9,10}, and the fuzzy subset is {NB, NM, NS, PS, PM, PB}.

The input and output membership functions and fuzzy control rules of the fuzzy controller 2 are shown in Fig. 9, Fig. 10 and Table II respectively.

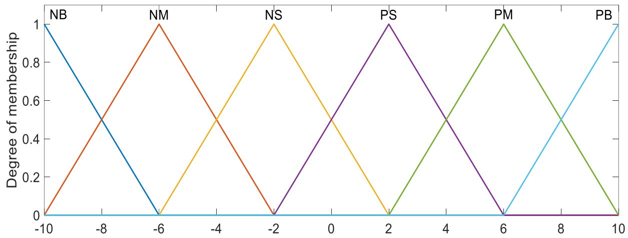

(a) Membership function of ΔSOC_b

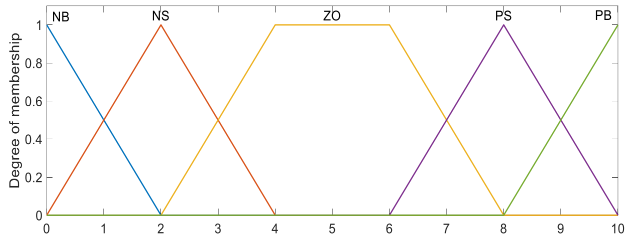

(b) Membership function of $SOC_b(t-1)$

Fig. 9. Fuzzy control input membership function

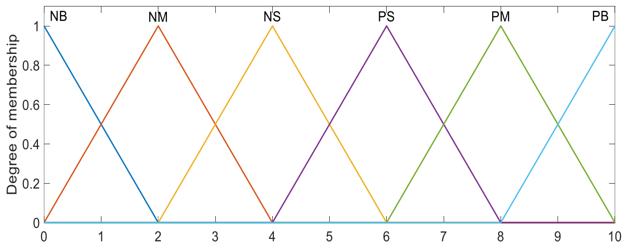

Fig. 10. Fuzzy control output membership function

Table II. Fuzzy control rule

ΔSOC_b	$SOC_b(t-1)$				
T	**NB**	**NS**	**ZO**	**PS**	**PB**
NB	NB	NM	NS	PS	PM
NM	NM	NS	PS	PM	PB
NS	NS	PM	PM	PB	PB
PS	PB	PB	PM	PM	NS
PM	PB	PM	PS	NS	NM
PB	PM	PS	NS	NM	NB

5. Simulation Analysis

the raw wind power output and the grid-connected power curve after wavelet packet-double fuzzy control are shown in Fig. 11;and the maximum power fluctuation rate before and after smoothing out power fluctuations for 1 and 10 minutes are shown in Fig. 12.

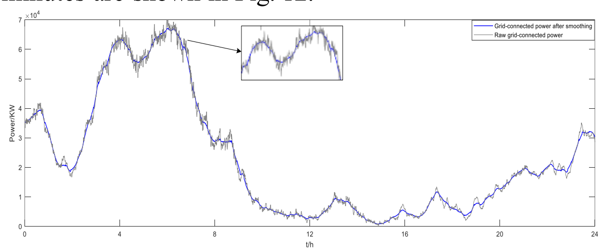

Fig. 11. Grid-connected power comparison

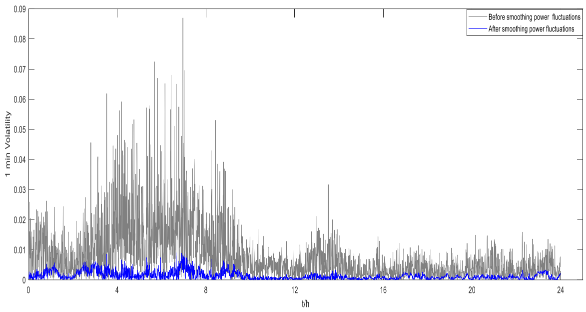

(a) 1 min volatility

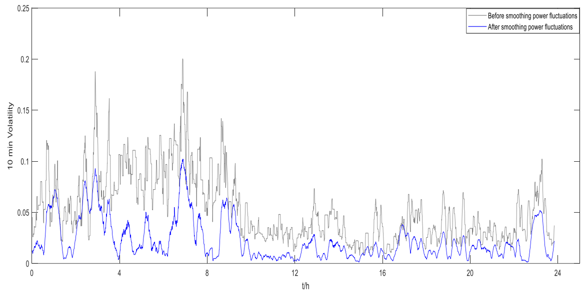

(b) 10 min volatility

Fig. 12. Comparison of 1 min and 10 min fluctuations before and after wind power leveling

Table III. Smoothing effect comparison

Method	1 min volatility		10 min volatility	
	Max	Min	Max	Min
Raw fluctuation	8.7%	0	20%	0.8%
Proposed method	0.9%	0	10.2%	0.1%

As can be seen from Fig.11, the grid-connected power after wavelet packet-double fuzzy control is smoother than the original wind power output power. From Fig.12, it can be seen that the fluctuation rate of grid-connected power after the introduction of hybrid energy storage wavelet packet-double fuzzy control smoothing is significantly lower than the fluctuation rate of grid-connected power of the original wind power output power on the time scale of 1min and 10min, which makes the grid-connected power of wind power smoother. As can be seen from Table III, the maximum value of the 1 min fluctuation rate of the original wind power output power in one day is 8.7%, and the maximum value of the 10 min fluctuation rate is 20%; the maximum and minimum values of the 1min fluctuation rate and 10 min fluctuation rate of the grid-connected power obtained by the wavelet packet decomposition method are smaller than the fluctuation rates of the original wind power output power in one day for 1 min and 10 min.

After the initial allocation of the original wind power output power by wavelet packet decomposition, a double fuzzy control algorithm is added to make a secondary correction to the allocated hybrid energy storage power in order to ensure that the state of charge of the supercapacitor and lithium battery remains within a reasonable range. A mathematical model was developed in MATLAB. Fig.13 shows the trend of the supercapacitor and battery charge states after the double fuzzy control algorithm is used compared to the trend of the change without the fuzzy control algorithm.

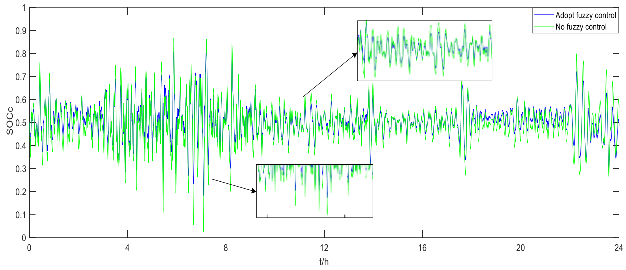

(a). Supercapacitor

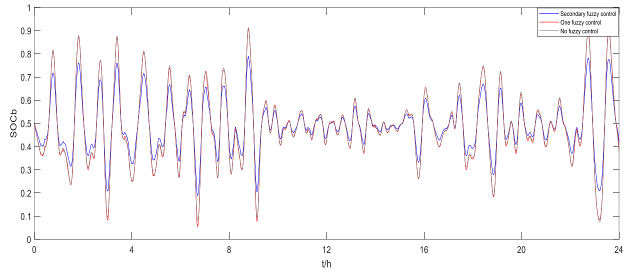

(b).Lithium battery

Fig. 13. Comparison of SOC variation trend of hybrid energy storage before and after fuzzy control

Table IV. Results contrast

SOC value	Control method	
	No fuzzy control	Use fuzzy control
SOC_b Min	0.08	0.19
SOC_b Max	0.91	0.79
SOC_c Min	0.02	0.18
SOC_c Max	0.86	0.79

As can be seen in Fig.13, when Li-ion battery SOC_b and supercapacitor SOC_c are not optimised using the fuzzy control algorithm, they are overcharged and discharged at certain times, which can have a significant impact on the life of the energy storage device. When Li-ion battery SOC_b and supercapacitor SOC_c are optimised using the fuzzy control algorithm, the trend is within a reasonable range and stays between 0.2 and 0.8 most of the time, keeping the Li-ion battery and supercapacitor in a safer state. At the same time, it can be seen that the lithium battery curve SOC_b after one fuzzy control This is due to the fact that Li-ion batteries are energy storage devices and when used in conjunction with supercapacitors, which are power storage devices, the capacity of Li-ion batteries is much greater than that of supercapacitors. Therefore, the optimization of supercapacitor SOC_c will have almost no effect on Li-ion battery SOC_b, thus increasing the lifetime of the supercapacitor while reducing the effect on Li-ion battery.

From Table IV, the maximum and minimum values of the supercapacitor charge state and the lithium battery charge state are within a reasonable range after using the dual fuzzy control algorithm. Therefore, the use of fuzzy control not only extends the service life of the energy storage device, but also improves the reliability and stability of the energy storage system.

The input and output fuzzy domains, fuzzy subsets and fuzzy rules of fuzzy control algorithm 2 were set to be the same as those of fuzzy algorithm 1 and analysed. Fig.14 shows a graph of the results of the modified fuzzy control algorithm 2 to optimise the SOC of the lithium battery, and Fig.15 shows the 1-minute and 10-minute fluctuations of grid-connected power after the modification of fuzzy control algorithm 2.

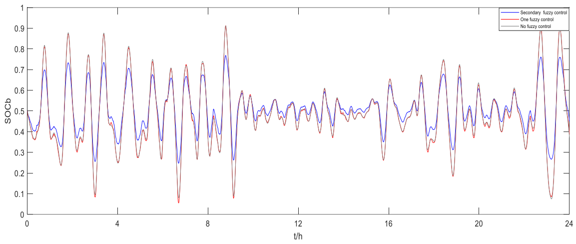

Fig. 14. The effect of optimizing the SOC of lithium battery after modifying fuzzy control algorithm 2

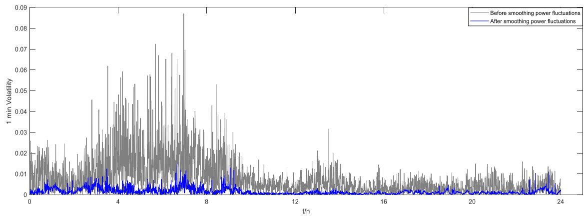

(b) 1 min volatility

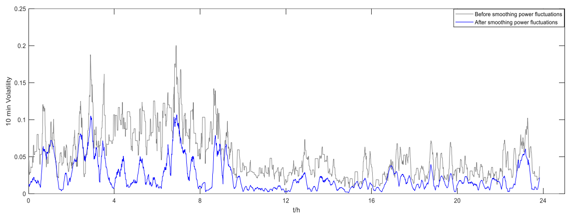

(b) 10 min volatility

Fig. 15. 1 minute and 10 minute volatility after modification of fuzzy control algorithm 2

As can be seen from Fig.14 and Fig.15, the modified fuzzy control algorithm 2 is more effective in optimising the lithium battery compared to the effect before the modification, with the minimum value of the lithium battery SOC becoming larger and the maximum value becoming smaller after the optimisation. However, this also means that the fluctuation component of grid connection increases, which makes the fluctuation rate of grid connection power at 1-minute and 10-minute time scales rise and not smooth, leading to a decrease in the effect of wind power fluctuation smoothing. Therefore, on balance, the pre-modified fuzzy control algorithm 2 is more effective in smoothing out wind power fluctuations based on optimised Li-ion battery SOC.

6. Conclusion

In this paper, a method based on wavelet packet-double fuzzy control for hybrid energy storage to smooth out wind power fluctuations is proposed. Combining the advantages of hybrid energy storage, the original output power of wind power is firstly decomposed by wavelet packet decomposition method to obtain the grid-connected power and the power allocated by hybrid energy storage; then the double fuzzy control algorithm is used to optimize the state of charge of supercapacitor and lithium battery, and the power allocated by hybrid energy storage is secondly modified to keep the state of charge of hybrid energy storage within a reasonable range to achieve the smoothing of wind power fluctuation.

The proposed wavelet packet-double fuzzy control method has a good effect on the suppression of wind power fluctuations. The use of fuzzy control algorithm for secondary correction of energy storage power not only optimises the power between hybrid energy storage devices, but also improves the safety and reliability of the operation of energy storage devices, providing a theoretical reference for the application of hybrid energy storage to smooth out wind power fluctuations. However, due to the limited laboratory conditions, the experimental prototype could not be built, and the research can only rely on simulation at present, and further efforts are needed in the future.

References

[1] Xue Yusheng, Lei Xing, and Xue Feng, "A Review on the Impact of Wind Power Uncertainty on Power Systems," Chinese Journal of Electrical Engineering (2014), vol. 34, no. 29, pp. 5029-5040.

[2] Li Peiqiang, Li Wenying, and Tang Jie, "A hybrid energy storage method to stabilize wind power fluctuations based on SOC optimization," Journal of Electric Power Systems and Automation (2017), vol. 29, no. 03, pp. 20-27.

[3] Tian Guizhen, Lu Dong, and Liu Guangchen, "Research on the Control Strategy of Hybrid Energy Storage to Suppress Direct Drive Wind Turbine Power Fluctuation Based on Zero-Phase Low-Pass Filter," Chinese Journal of Solar Energy (2021), vol. 42, no. 06, pp. 72-78.

[4] Liu Zhongmin, Qi Guoyuan, and Gao Jinggeng, "Strategy for Hybrid Energy Storage System to Stabilize Power Fluctuations in Wind and Solar Power Generation," Power Electronics Technology (2021), vol. 55, no. 11, pp. 64-67.

[5] Lei Yong, and Lin Xiaodong, "Application of superconducting magnetic energy storage-battery hybrid energy storage system in smoothing power fluctuations of wind farms," High Voltage Technology (2019), vol. 45, no. 03, pp. 983 -992.

[6] Zhang Qing, Li Xinran, and Yang Ming, "Hybrid energy storage capacity allocation method with the greatest net benefit to stabilize wind power fluctuations," Journal of Electrotechnical Technology (2016), vol. 31, no. 14, pp. 40-48 .

[7] Y. Sun et al., "Model predictive control and improved low-pass filtering strategies based on wind power fluctuation mitigation," Journal of modern power systems and clean energy (2018), vol. 7, no. 3, pp . 512-524, . doi: 10.1007/s40565-018-0474-5.

[8] Han Xiaojuan, Chen Yueyan, and Zhang Hao, "Application of Hybrid Energy Storage Technology Based on Wavelet Packet Decomposition in Wind Farm Power Fluctuation," Chinese Journal of Electrical Engineering (2013), vol. 33, no. 19, pp. 8-13+24.

[9]Jie Wu, Ming Ding " Hybrid energy storage smoothing control strategy for wind power fluctuations using adaptive wavelet packet decomposition," Power System Automation (2017), vol. 41, no. 03, pp. 7-12.

[10].Zhang Baoming, Chen Jie, and Fu Juxia, "Wind power fluctuation control strategy based on wavelet packet hybrid energy storage system". Electrical Machines and Control Applications(2020), vol. 47, no. 03, pp. 75-80+94.

[11] Jia Weiqing, Ren Yongfeng, and Xue Yu, "Hybrid energy storage based on wavelet packet-fuzzy control to stabilize power fluctuations of large wind farms," Journal of Solar Energy (2021), vol. 42, no. 09, pp. 357-363 .

[12] Wang Supeng, Zhang Xinhui, and Wu Wenhao, "Hybrid energy storage selection and capacity optimization configuration method for wind power suppression," Smart Power (2021), vol. 49, no. 09, pp. 16-23.